

Interlayer exchange coupling and magnetic anisotropy in prototype trilayers: *Ab initio* theory versus experiment

R. Hammerling,* J. Zabloudil, and P. Weinberger

Center for Computational Materials Science, Technical University, Getreidemarkt 9/134, A-1060 Vienna, Austria

J. Lindner,† E. Kosubek, R. Nünthel, and K. Baberschke

Institut für Experimentalphysik, Freie Universität Berlin, Arnimallee 14, D-14195 Berlin, Germany

(Received 28 March 2003; published 16 September 2003)

The magnetic anisotropy energy (MAE) and the interlayer exchange coupling (IEC) of prototype $\text{Cu}_4\text{Ni}_8\text{Cu}_N\text{Ni}_9/\text{Cu}(001)$ trilayers are calculated using an *ab initio* approach based on the experimental lattice spacings. The results thereof are compared to ferromagnetic resonance experiments which allow for the quantitative determination of the MAE as well as the IEC. The tetragonal distortion of the Ni films due to the pseudomorphic growth leads to a positive MAE of the inner Ni layers favoring an out-of-plane easy axis. At the Cu/Ni interfaces a negative surface anisotropy is present which is, however, reduced compared to a Ni/vacuum interface. The MAE is clearly determined by the Ni layers only, whereas the IEC is shown to result from Ni and Cu layers at the inner Cu/Ni interfaces.

DOI: 10.1103/PhysRevB.68.092406

PACS number(s): 75.70.Cn, 76.50.+g

Nowadays it is well known that ultrathin ferromagnetic layers separated by a nonmagnetic spacer layer may interact via the so-called interlayer exchange coupling (IEC). This interaction was found to oscillate between ferromagnetic (FM) and antiferromagnetic (AFM) alignments as a function of the spacer thickness. The IEC defined as the difference between the free energy for FM and for AFM coupling has been the subject of many studies. The theoretical understanding of the phenomenon nowadays mostly relies on model calculations. The most frequently used picture is probably the Ruderman-Kittel-Yosida (Refs. 1,2) model which explains the observed oscillation periods to arise from extremal spanning vectors of the Fermi surface (the so-called calipers) of the spacer material. The magneto-optical Kerr effect (MOKE), most widely used, and other static magnetometries usually yield values of the coupling only for AFM coupled layers, whereas for FM coupling, in most cases, no results can be obtained. A method which is capable of such a determination and sensitive enough to measure down to the monolayer (ML) limit is the ferromagnetic resonance (FMR).^{3,4}

In this paper we present simultaneously a theoretical and an experimental study on prototype $\text{Cu}_4\text{Ni}_8\text{Cu}_N\text{Ni}_9/\text{Cu}(001)$ trilayers with the focus on the behavior for small spacer thicknesses in the range $N=2-10$ ML. The Ni/Cu(001) system can be viewed as a prototype system, since it implements structural as well as magnetic homogeneity. Details concerning the film preparation under ultrahigh vacuum conditions have been discussed elsewhere.⁴⁻⁷ A hard-sphere model of the trilayers is shown in Fig. 1(a). In order to have a limited set of parameters, only N was varied between the different trilayer systems, whereas the thicknesses of the Ni films were kept constant (8 and 9 ML, respectively). Ni films grow pseudomorphically up to at least 15 ML adopting the Cu in-plane lattice constant. In the vertical growth direction this leads to a contraction of the Ni film. A quantitative I/V-low-energy electron diffraction (LEED) study⁸ revealed values of $2.53(2)$ Å for the in-plane nearest-neighbor distance

and $1.70(2)$ Å for the interlayer separation. Relative to the Cu-bulk interlayer distance of 1.805 Å this means a contraction of about -5.5% (if referred to the Ni-bulk value of 1.76 Å its value amounts to -3.2%). The question whether the pseudomorphic growth continues upon capping the Ni film with the Cu spacer and, moreover, when the second Ni film is deposited on top of the spacer has not been discussed in Ref. 8. Since the structure is an important input for theory, this question is—in the present work—addressed via I/V-LEED experiments carried out after each evaporation step. The I/V-LEED spectra recorded for the specular reflected (00) beam during the stepwise preparation of a $\text{Ni}_8\text{Cu}_6\text{Ni}_9/\text{Cu}(001)$ trilayer are shown in Fig. 1(b). From the position of the Bragg peaks one can extract the averaged vertical interlayer distance. If, on the other hand, the interlayer distance is known—as in the case of the Cu(001) substrate—relative shifts of the Bragg peaks can be translated directly into changes of the vertical layer separation. A shift to higher (lower) energy values indicates a contraction (expansion) of the interlayer distance. Clearly such a shift of the intensity maxima towards *higher* energies can be observed after the Ni_9 film is deposited. This shift shows the

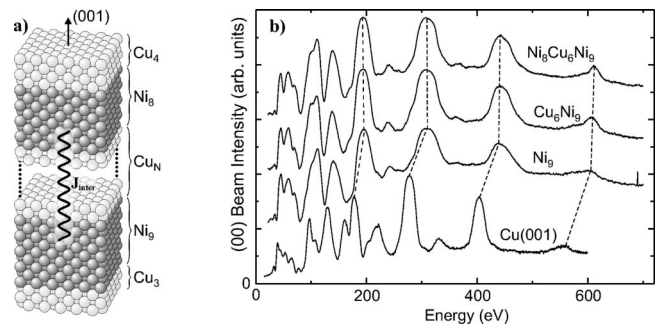


FIG. 1. (a) Hard-sphere model of the $\text{Cu}_4\text{Ni}_8\text{Cu}_N\text{Ni}_9/\text{Cu}(001)$ trilayers. (b) I/V-LEED spectra taken from the specular reflected (00) beam for (from bottom to top) Cu(001), Ni_9 , Cu_6Ni_9 , and $\text{Ni}_8\text{Cu}_6\text{Ni}_9$.

vertical contraction of the Ni film discussed already in (Ref. 8). No changes in the maxima are found after the evaporation of the Cu spacer and the topmost Ni film. Thus, one can conclude that the contraction of -5.5% is present within the whole trilayer.

The magnetic anisotropy of the trilayers can phenomenologically be described by the part of the free energy E per unit area being anisotropic with respect to the directions of the magnetizations \vec{M}_1 and \vec{M}_2 in the two films

$$E = \sum_{i=1}^2 (2\pi M_i^2 - K_{2\perp,i}) d_i \cos^2 \theta_i - J_{inter} \frac{\vec{M}_1 \cdot \vec{M}_2}{M_1 M_2}. \quad (1)$$

Here the d_i are the thicknesses of the individual Ni slabs, $2\pi M_i^2$ is the shape anisotropy due to dipole-dipole interaction, and $K_{2\perp,i} = K_{2\perp,i}^V + (K_{2\perp,i}^{S1} + K_{2\perp,i}^{S2})/d_i$ denotes the intrinsic uniaxial anisotropy which can be split into a part arising from the film volume ($K_{2\perp,i}^V$) and a contribution from the two surfaces ($K_{2\perp,i}^{S1}$ upper surface, $K_{2\perp,i}^{S2}$ lower surface). In the following we set $S_1 = S_2 = S$ as our Ni films face Cu on both sides. The angles θ_i measure the magnetization directions with respect to the film normal. For $2\pi M_i^2 - K_{2\perp,i} > 0$ (< 0) the easy axis of magnetization lies in (out of) the film plane. Within the framework of Eq. (1) the IEC corresponds to the *macroscopic* coupling constant J_{inter} .² The magnetic anisotropy energy is defined as the energy difference between in- and out-of-plane orientations of the magnetization, i.e., magnetic anisotropy energy (MAE) = $E(\theta_i = \pi/2) - E(\theta_i = 0)$. Ultrathin Ni films on Cu(001) present a reorientation of the easy axis of the magnetization from in to out of plane⁹ which at room temperature occurs at about 10–11 ML.¹⁰ Upon capping the Ni film with Cu the reorientation thickness is reduced to about 7–8 ML.¹⁰ Consequently, both Ni films in our trilayers exhibit an out-of-plane easy axis.⁷ This configuration was chosen because of enabling one to carry out additional MOKE measurements in the most sensitive polar geometry.⁷ The magnetic anisotropy energies as well as the coupling between the two films were determined by means of *in situ* FMR at a microwave frequency of 9 GHz and external magnetic fields up to 15 kOe. Using *in situ* FMR the trilayer can be grown *and* measured within a step-by-step experiment: First, the bottom Ni₉ film capped with the Cu_N spacer layer is evaporated and investigated while in a second step, the topmost Cu₄Ni₈ layers are deposited. This approach allows to “switch on” the IEC within the second step and monitor its influence on the FMR signal of the bottom Ni₉ film. Via angular dependent FMR measurements, i.e., by varying the θ_i angles of the two magnetizations \vec{M}_i , before and after the deposition of the topmost layers, one can separate the magnetic anisotropies being proportional to $\cos^2 \theta_i$ [first term in Eq. (1)] from J_{inter} which scales with $\cos(\theta_1 - \theta_2)$ [second term in Eq. (1)]. A detailed description of this procedure yielding absolute values for J_{inter} was described previously.^{5–7} The measurements were performed in a temperature range of 50–400 K which covers almost the whole range from the low-temperature regime up to the Curie temperature.

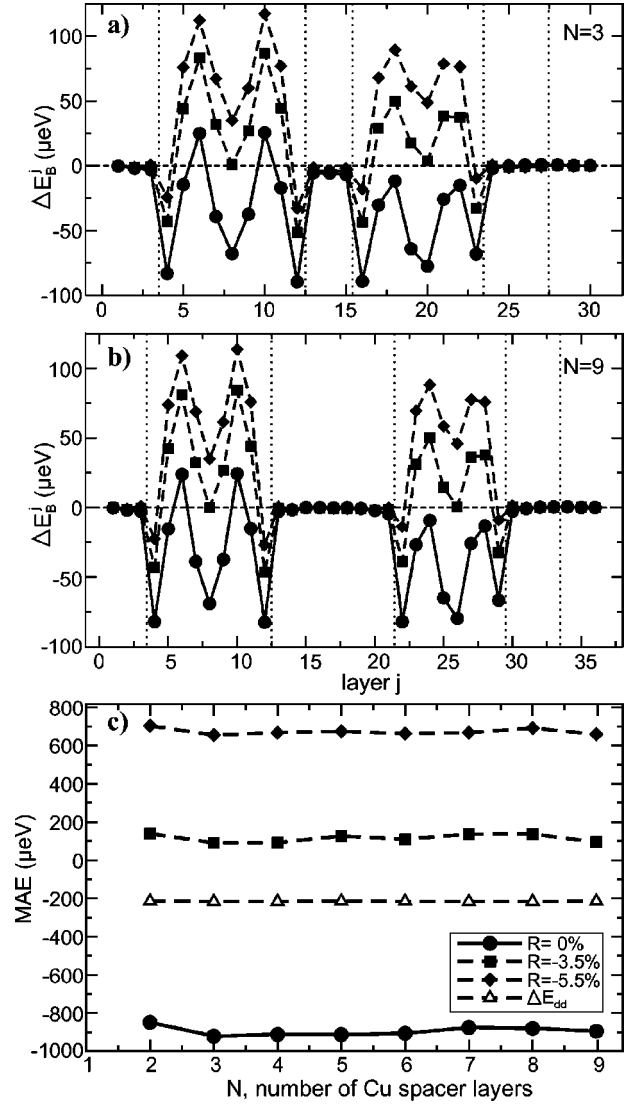


FIG. 2. Layer-resolved band energy difference ΔE_B for a trilayer with (a) $N=3$ and (b) $N=9$. (c) MAE as a function of the spacer layer thickness N for the different vertical relaxations.

In using the relativistic spin-polarized screened Korringa-Kohn-Rostoker method for layered systems, the theoretical aspects of which are discussed in detail in Ref. 11, the calculations were carried out for the same type of trilayers on which the FMR experiments have been done, namely, those shown in Fig. 1(a). For the calculations shown in Fig. 2 different (uniform) vertical relaxations of 0% (circles), -3.5% (squares), and -5.5% (diamonds) of the trilayers with respect to the Cu(001) substrate were assumed, the lattice spacing *within* the layers always being that of Cu bulk. Three buffer layers of Cu were found to be sufficient to guarantee reliable matching to the semi-infinite Cu(001) substrate; at least two vacuum layers were used to join up to the semi-infinite vacuum. The MAE is calculated as the sum of differences in the magnetic dipole-dipole energy ΔE_{dd} and in the band energy ΔE_B (intrinsic contribution) between a uniform in-plane and a uniform out-of-plane orientation of the magnetization. The layer-resolved band energy differences for trilayers with $N=3$ and $N=9$ are presented in Figs. 2(a)

TABLE I. Volume and surface anisotropy constants ($\mu\text{eV}/\text{atom}$) for Ni/Cu(001) at $T=0$ K. Note that the results from Ref. 10 were measured at room temperature.

	$K_{2\perp,i}^V$	$K_{2\perp,i}^{\text{Ni/Cu}}$	$K_{2\perp,i}^{\text{Ni/vacuum}}$
Experiment	70(20) (Ref. 16)	-60(10) (Ref. 10)	-100(20) (Refs. 10,16)
Theory	80(20)	-20(10)	-100(20) (Ref. 15)

and 2(b). The layer numbering starts at the three Cu buffer layers and comprises the trilayer itself, the four Cu capping layers, and three vacuum layers [the different films within the slab are separated by dotted lines in Figs. 2(a) and 2(b)]. One obtains the following results: (i) A sizeable anisotropy energy only arises from the Ni layers. (ii) The Ni layers facing Cu layers show a negative contribution, thus favoring an in-plane easy axis. (iii) Only the volume part of the Ni film presents a positive anisotropy contribution for the case that the experimentally derived distortion of -5.5% in the film is assumed. From this it follows that in order to explain the experimentally observed positive overall MAE (Ref. 7) the lattice relaxation has to be taken into account. In Fig. 2(c) the MAE is plotted as a function of N for the three different distortions. Note that each data point in Fig. 2(c) corresponds to the sum of ΔE_B over all layers including the dipole-dipole energy ΔE_{dd} shown in this figure as triangles. As can be seen a positive MAE is only revealed for the distorted systems. Furthermore, the MAE shows no dependence on the spacer thickness N . Unlike for many other systems the shape anisotropy given by ΔE_{dd} in the investigated system is too small to lead to a negative overall MAE and thus ΔE_B dominates resulting in a MAE > 0 . Dividing the theoretical value of ΔE_{dd} by the number of Ni layers yields an energy per atom, which amounts to a value of $12.7 \mu\text{eV}/\text{atom}$ for $2\pi M$.² As compared to the experimental value for Ni bulk at $T=0$ K, namely, $12.1 \mu\text{eV}/\text{atom}$, this indicates that the Ni moments and thus the magnetization are on the average bulklike. This behavior was experimentally verified via an *in situ* Superconducting quantum interference device investigation which showed that only for Ni thicknesses smaller than 5 ML a decrease of the $T=0$ K magnetization with respect to the bulk value occurs.¹²

In order to compare the theoretical results to the experimentally determined second-order constants given by Eq. (1) one has to identify the energy of the interface Ni layers with the surface anisotropy $K_{2\perp}^S$ and the sum of the energy of the interior Ni layers divided by their number with the volume contribution $K_{2\perp}^V$. As can be seen from Table I a very good agreement between theory and experiment concerning $K_{2\perp}^V$ applies. The experimental value for $K_{2\perp}^{\text{Ni/Cu}}$, however, is by about a factor of 2–3 larger than found theoretically. This discrepancy most likely results from surface roughness and/or interface mixing which was not taken into account in the calculations. The driving force for the perpendicular orientation of the Ni films is therefore the positive volume contribution due to the tetragonal distortion. The surface anisotropy of the Ni/Cu interface—though still being negative—is

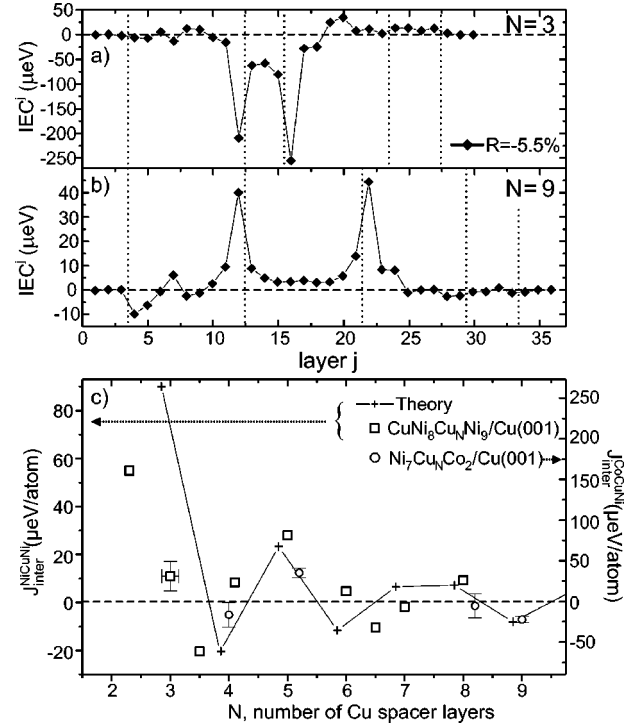


FIG. 3. Layer-resolved IEC for a trilayer with (a) $N=3$ and (b) $N=9$. In (c) the experimental results for both trilayer systems, indicated by the open squares and circles, are plotted as function of the numbers of spacer layers N . The theoretical IEC values (crosses) have been upshifted on the x axis by 0.7 ML (see text).

reduced with respect to Ni/vacuum which explains the smaller reorientation thicknesses found for Cu capped Ni films.¹⁰

Now we turn to the IEC. In Figs. 3(a) and 3(b) the calculated layer-resolved IEC for the experimental lattice relaxation of -5.5% is plotted for two spacer thicknesses of $N=3$ and $N=9$, the layer numbering being the same as in Fig. 2. The main contribution to the IEC stems from Ni and Cu layers at or close to the Ni/Cu interface. For $N=3$ ($N=9$) the overall IEC energy is < 0 (> 0) indicating AFM (FM) coupling. Figure 3(c) shows the results of the experimental determination of the IEC for the $\text{Cu}_4\text{Ni}_8\text{Cu}_N\text{Ni}_9/\text{Cu}(001)$ trilayers (open squares) with N ranging from 2–10. The experimental values for the $\text{Cu}_4\text{Ni}_8\text{Cu}_N\text{Ni}_9/\text{Cu}(001)$ system ranging from $J_{\text{inter}}=0$ to about $60 \mu\text{eV}/\text{atom}$ were extrapolated to $T=0$ K in order to compare them to the theoretical calculations. This extrapolation was done using a $1-(T/T_C)^{3/2}$ functional dependence of the IEC which was shown to correctly describe the temperature dependence of the IEC for various systems.⁶ In addition to the $\text{Cu}_4\text{Ni}_8\text{Cu}_N\text{Ni}_9/\text{Cu}(001)$ trilayers, results for $\text{Ni}_7\text{Cu}_N\text{Co}_2/\text{Cu}(001)$ trilayers (open circles) are added. Note that the experimentally determined values for the IEC are by about a factor of 3 larger for the $\text{Ni}_7\text{Cu}_N\text{Co}_2/\text{Cu}(001)$ systems (right y axis compared to the left one). For a detailed discussion of the $\text{Ni}_7\text{Cu}_N\text{Co}_2/\text{Cu}(001)$ systems, see (Refs. 6 and 7). An oscillatory behavior is clearly seen for both systems, indicating that—except the strength—the overall behavior is not influenced upon substituting one Ni film with

Co. The oscillations are also found in the *ab initio* calculation shown as crosses. However, in order to obtain the best agreement with the experiment the theoretical curve has to be upshifted by 0.7 ML, which in turn indicates that the effective experimental thickness seems to be by 0.7 ML smaller than the nominal evaporation rate. This can easily be understood considering a small amount of interdiffusion occurring during the film growth, a fact that is well known to happen for Ni as well as Co/Cu(001).¹³ In principle, interdiffusion effects can theoretically be taken into account in terms of the inhomogeneous Coherent Potential Approximation, see, e.g., (Ref. 14). The profile, however, can only serve as a parametric, qualitative description as long as no reliable experimental data to compare with are available.

Although the principal behavior of the IEC found experimentally is reproduced by the theory, the absolute strength of the coupling calculated¹¹ for the $\text{Cu}_4\text{Ni}_8\text{Cu}_N\text{Ni}_9/\text{Cu}(001)$ trilayers has to be scaled by a factor of 1/10 to match the experimental values. It should be noted, however, that experimentally one makes use of Eq. (1), i.e., of a “macroscopic” Heisenberg ansatz. The fact that the calculated values are larger than those obtained from this procedure indicates that the “experimental” J_{inter} displayed in Fig. 3 not necessarily is identical to the *microscopical* IEC. Only a thermodynamically averaged Heisenberg model would eventually lead to an expression as the one introduced in Eq. (1):

$$\begin{aligned} \langle E \rangle &= \left\langle \sum_{i,j} J_{ij} \frac{\vec{m}_i \cdot \vec{m}_j}{m_i m_j} \right\rangle \sim \left\langle J \sum_{i,j} \frac{\vec{m}_i \cdot \vec{m}_j}{m_i m_j} \right\rangle \\ &\sim \langle J \rangle \left\langle \sum_{i,j} \frac{\vec{m}_i \cdot \vec{m}_j}{m_i m_j} \right\rangle \rightarrow J_{inter} \frac{\vec{M}_1 \cdot \vec{M}_2}{M_1 M_2}. \end{aligned} \quad (2)$$

In Eq. (2) the \vec{m}_i refer to magnetic moments at sites i and J_{ij}

is the coupling energy between two such moments. Clearly enough also interface roughness not included in the theoretical description adds to the discrepancy in amplitudes between theory and experiment. This becomes evident by considering the fact shown in Fig. 3 that the IEC mainly arises from the interfaces of the films. The phases of the oscillations, however, can be expected to be in good agreement since in both cases the switching between two macroscopic magnetic configurations is mapped.

In summary we have shown for the case of prototype $\text{Cu}_4\text{Ni}_8\text{Cu}_N\text{Ni}_9/\text{Cu}(001)$ trilayers that a combination of experiment and *ab initio* theory yields a better understanding of fundamental magnetic properties such as the MAE and the IEC. Due to the included tetragonal distortion the results show a quantitative agreement for the volume contribution of the Ni films and thus lead to the experimentally observed easy axis perpendicular to the film plane. The surface anisotropy is negative and strongly reduced if the Ni films are capped by a Cu overlayer. Unlike the MAE which is determined by the Ni layers only and independent of the coupling between the Ni films, the IEC is strongly influenced by the Ni and Cu interface layers. The calculations reproduce the oscillatory behavior and the very strong dependence of the number of atomic spacer layers. As discussed above, namely, because of inherent conceptual differences, the theoretical IEC will not be identical to the experimental J_{inter} (projected on a Heisenberg Hamiltonian, influence of interface roughness and/or interface mixing); nevertheless the numerical agreement can be expected to be very good.

This work was supported by the Fonds zur Förderung der wissenschaftlichen Forschung (Project No. W004), the Austrian Ministry of Science (Project No. GZ 45.490), and by the DFG Sfb290, TP A2. K. Lenz is thanked for helpful discussions.

*Electronic address: babgroup@physik.fu-berlin.de

†Corresponding author. FAX: +49-30-838-53646.

¹M.D. Stiles, Phys. Rev. B **48**, 7238 (1993), and references therein.

²P. Bruno, Phys. Rev. B **52**, 411 (1995), and references therein.

³M. Farle, Rep. Prog. Phys. **61**, 755 (1998).

⁴J. Lindner, Z. Kollonitsch, E. Kosubek, M. Farle, and K. Baberschke, Phys. Rev. B **63**, 094413 (2001).

⁵J. Lindner and K. Baberschke, J. Magn. Magn. Mater. **240**, 220 (2002).

⁶J. Lindner, C. Rüdert, E. Kosubek, P. Pouloupoulos, K. Baberschke, P. Blomquist, and R. Wäppling, D.L. Mills, Phys. Rev. Lett. **88**, 167206 (2002).

⁷J. Lindner and K. Baberschke, J. Phys.: Condens. Matter **15**, S465 (2003); **15**, R193 (2003).

⁸W. Platow, U. Bovensiepen, P. Pouloupoulos, M. Farle, K. Baberschke, L. Hammer, S. Walter, S. Müller, and K. Heinz, Phys. Rev. B **59**, 12 641 (1999).

⁹K. Baberschke, in *Bandferromagnetism*, edited by K. Baberschke,

M. Donath, and W. Nolting (Springer-Verlag, Berlin, 2001), and references therein.

¹⁰J. Lindner, P. Pouloupoulos, R. Nünthel, E. Kosubek, H. Wende, and K. Baberschke, Surf. Sci. **523**, L65 (2003).

¹¹P. Weinberger and L. Szunyogh, Comput. Mater. Sci. **17**, 414 (2000).

¹²A. Ney, A. Scherz, P. Pouloupoulos, K. Lenz, H. Wende, K. Baberschke, F. Wilhelm, and N.B. Brookes, Phys. Rev. B **65**, 024411 (2002).

¹³J. Fassbender, R. Allenspach, and U. Dürig, Surf. Sci. **383**, L742 (1997); J. Lindner, P. Pouloupoulos, F. Wilhelm, M. Farle, and K. Baberschke, Phys. Rev. B **62**, 10 431 (2000).

¹⁴H.C. Herper, P. Weinberger, L. Szunyogh, and C. Sommers, Phys. Rev. B **66**, 064426 (2002).

¹⁵C. Uiberacker, J. Zabloudil, P. Weinberger, L. Szunyogh, and C. Sommers, Phys. Rev. Lett. **82**, 1289 (1999).

¹⁶M. Farle, B. Mirwald-Schulz, A.N. Anisimov, W. Platow, and K. Baberschke, Phys. Rev. B **55**, 3708 (1997).